

Effect of CuO particle size on synthesis temperature and microstructure of $\text{Al}_2\text{O}_3\text{p}$ –Al composites from Al–CuO system

Ge ZHAO, Zhi-ming SHI, Na TA, Rui-ying ZHANG

School of Materials Science and Engineering, Inner Mongolia University of Technology, Hohhot 010051, China

Received 17 October 2014; accepted 24 October 2014

Abstract: $\text{Al}_2\text{O}_3\text{p}$ –Al composites were synthesized using an in-situ reaction in the 80%Al–20%CuO (mass fraction) system. The effects of the CuO particle size on the synthesis temperature and microstructure of the composites were investigated by various methods. The results indicate that the CuO particle size has a significant effect on the temperature at which the complete reaction in the Al–CuO system occurs: the temperature is 200 °C lower in the Al–CuO system containing CuO particles with sizes less than 6 μm than that containing CuO particles with sizes less than 100 μm . The interfacial bonding between Al_2O_3 particles and Al is not complete when the temperature is below a critical value. The morphology of the Al_2O_3 particles varies from ribbon-like shape to near spherical shape when the temperature is above a critical value. These two critical temperatures are affected by the particle size of CuO, and the critical temperature of the sample containing CuO particles with sizes less than 6 μm is 100 °C lower than that of the sample containing CuO particles with sizes less than 100 μm .

Key words: CuO; particle size; synthesis temperature; $\text{Al}_2\text{O}_3\text{p}$ –Al composite

1 Introduction

Particle-reinforced aluminum matrix composites are of interest because of their highly desirable properties, such as high specific strength and stiffness, good wear resistance, low thermal expansion coefficient and traditional preparation process, for various applications in the aerospace, military, electronic devices and automobile industries [1–3]. Traditionally, composites are produced directly by adding reinforcement particles to the aluminum matrix using ex-situ techniques. In contrast, the in-situ technique is extensively utilized to produce particle-reinforced composites with contaminant-free reinforcement/matrix interfaces because the reinforcement particles are formed by the nucleation and growth from the parent matrix phase [4]. The in-situ formation of particles also provides effective control of the particle size and the level of the reinforcement, yielding better tailorability of properties [5].

The chemical reactions between the reactants, which are keys to the production of in-situ metal matrix composites, are extremely important. The displacement reactions between Al and metal oxides, such as CuO [6], SiO_2 [7], ZnO [8] and TiO_2 [9], used to produce

$\text{Al}_2\text{O}_3\text{p}$ –Al composites have been widely discussed due to the low cost of raw materials. CuO is one of the most widely used metal oxides because it easily reacts with aluminum. An Al_2O_3 –Al(Cu) composite was synthesized in the CuO–Al system at 1173 K by inserting the samples into the molten aluminium [10]. Some Cu_2O phase still existed in the CuO–Al system after being sintered at 950 °C for 30 min [11]. An increase in the sintering time accelerated the formation of submicron in-situ α - Al_2O_3 particles and decreased the quantity of the Al_2Cu intermetallic phase [12]. The Al_2O_3 particle size was observed to increase with increasing temperature and oxidation time [13]. Below 700 °C, amorphous alumina formed, which transformed to crystalline alumina at higher temperatures [14]. The initial reaction temperatures increased with an increase in the heating rate [15]. The eutectic network in the oil-quenched sample was distributed more uniformly and was finer in size than that of the furnace-cooled sample when the sintered sample was cooled down from 1000 °C [16]. These studies indicate that the microstructure of the composite is controlled by the process parameters in the Al–CuO system.

However, the effect of the CuO particle size on the microstructure of the composite has not been extensively

investigated. A change in the size of low melting component is found to have a limited influence on the synthesis conditions. However, a change in the size of high melting component size influences the combustion temperature and propagation velocity [17]. Therefore, in this study the effects of the CuO particle size on the composite microstructure, specifically on the morphology of in-situ Al₂O₃ particles and the interface bonding between Al₂O₃ particles and Al at different synthesized temperatures, were investigated, which is beneficial to obtaining a strong interface bonding between the in-situ Al₂O₃ particles and Al and to obtaining a high performance Al₂O₃_p-Al composite.

2 Experimental

The powder mixture containing 80% Al and 20% CuO (mass fraction) were used to prepare the in-situ composite. Two different kinds of CuO (referred to as samples 1 and 2, AR) and one kind of Al powder (< 20 μm, AR) were used as the raw materials. The particle sizes of CuO powders were less than 100 μm and 6 μm for samples 1 and 2, respectively. Each powder mixture was blended and cold-pressed under 400 MPa to form a compact with a diameter of 10 mm.

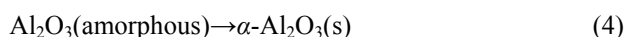
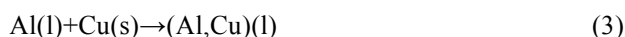
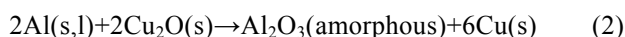
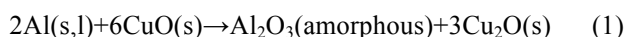
Differential scanning calorimetry (DSC, Netzsch STA409 PC) measurement was conducted to determine the reaction temperatures between Al and CuO. During the analysis, two samples (*d* 4.0 mm×1.0 mm) obtained from two different (CuO+Al) green compacts (corresponding to two different CuO powders) were used. These two samples were heated in argon atmosphere in the differential scanning calorimeter where the temperature increased from ambient to 900 °C at a heating rate of 20 °C/min.

The reactions of these two different (CuO+Al) green compacts were performed by directly placing them into a tube furnace at 600, 700, 800 and 900 °C and sintered for 1 h in argon atmosphere. To further analyze the effect of the particle size of CuO on the microstructure of products, two other different green compacts were sintered at 1000 °C. All samples were allowed to cool down to room temperature inside the furnace with the power turned off. The main phase analysis of the composite and the compact was identified by X-ray diffraction (XRD, D/MAX-2500/PC, 40 kV, 20 mA) techniques using Cu K_α radiation. The microstructures of all the samples were studied by optical microscopy and scanning electron microscopy (SEM). Elemental chemical analysis was performed by using an energy dispersive spectrometer (EDS) attached to the SEM.

3 Results and discussion

3.1 DSC results

Figure 1 shows the DSC curves of samples 1 and 2. The DSC curve of sample 1 is observed to exhibit three peaks, one endothermic peak at approximately 680 °C due to the melting of Al and two exothermic peaks between 570 °C and 760 °C, which are located on the left and right sides of the endothermic peak and are overlapping the endothermic peak. The DSC curve of sample 2 is similar to that of sample 1 when the temperature is below 760 °C, but the Al melts at a relatively low temperature in sample 1 compared with that in sample 2. However, another independent exothermic peak was observed at 810–870 °C for DSC curve of sample 2. According to Refs. [5,12,14,16,18,19], the peak is explained by Reactions (1)–(4) in Ref. [16]:



According to the above analysis, it is reasonable to postulate that the CuO particle size can influence the heat release during the reaction between Al and CuO. Fine CuO particles have larger available reacting surface areas, which leads to the violent reaction. BISWAS et al [20] reported a similar effect of the particle size of Ni on the thermal response of an Al/Ni system. The violent reaction corresponds to a higher heat release rate. This can explain the relatively low melting temperature of Al and the appearance of the third exothermic peak in the DSC curve of sample 2.

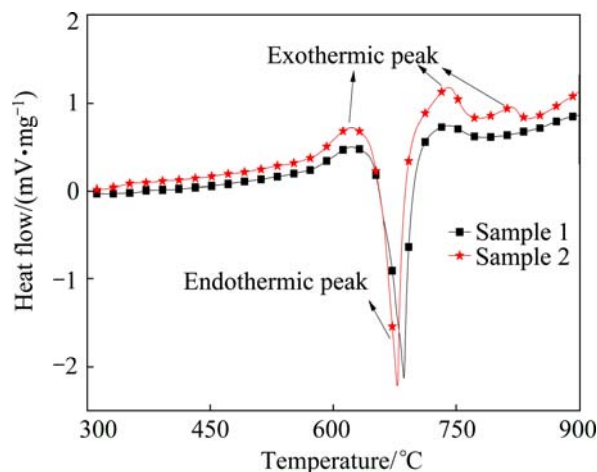


Fig. 1 DSC curves of Al-20%CuO samples obtained under flowing argon at heating rate of 20 °C/min

3.2 XRD results

Figure 2 shows XRD patterns of the green sample and the sintered samples. Only peaks that correspond to Al and CuO are found in the pattern of the green sample. The phases of Cu_2O , Cu and Al are detected in sample 1 sintered below $700\text{ }^\circ\text{C}$ and sample 2 sintered at $600\text{ }^\circ\text{C}$, and the representative XRD result of sample 2 sintered at $600\text{ }^\circ\text{C}$ is shown in Fig. 2(b). Figure 2(c) shows that Cu, Al_2Cu and $\alpha\text{-Al}_2\text{O}_3$ appear in the sample sintered at $800\text{ }^\circ\text{C}$ (sample 1). In the patterns of all of the other sintered samples, peaks that correspond to Al, Al_2Cu and $\alpha\text{-Al}_2\text{O}_3$ were identified. Interestingly, the complete

reaction between Al and CuO can be achieved in the sample sintered at $700\text{ }^\circ\text{C}$ (sample 2), as shown in the XRD pattern in Fig. 2(d). This analysis indicates that the chemical reactions between Al and CuO are strongly influenced by the particle size of the CuO powders.

3.3 Microstructure

3.3.1 Green samples

The microstructures of Al–20%CuO green samples are shown in Fig. 3. The bright CuO powders are distributed between the Al particles, which form the dark Al matrix.

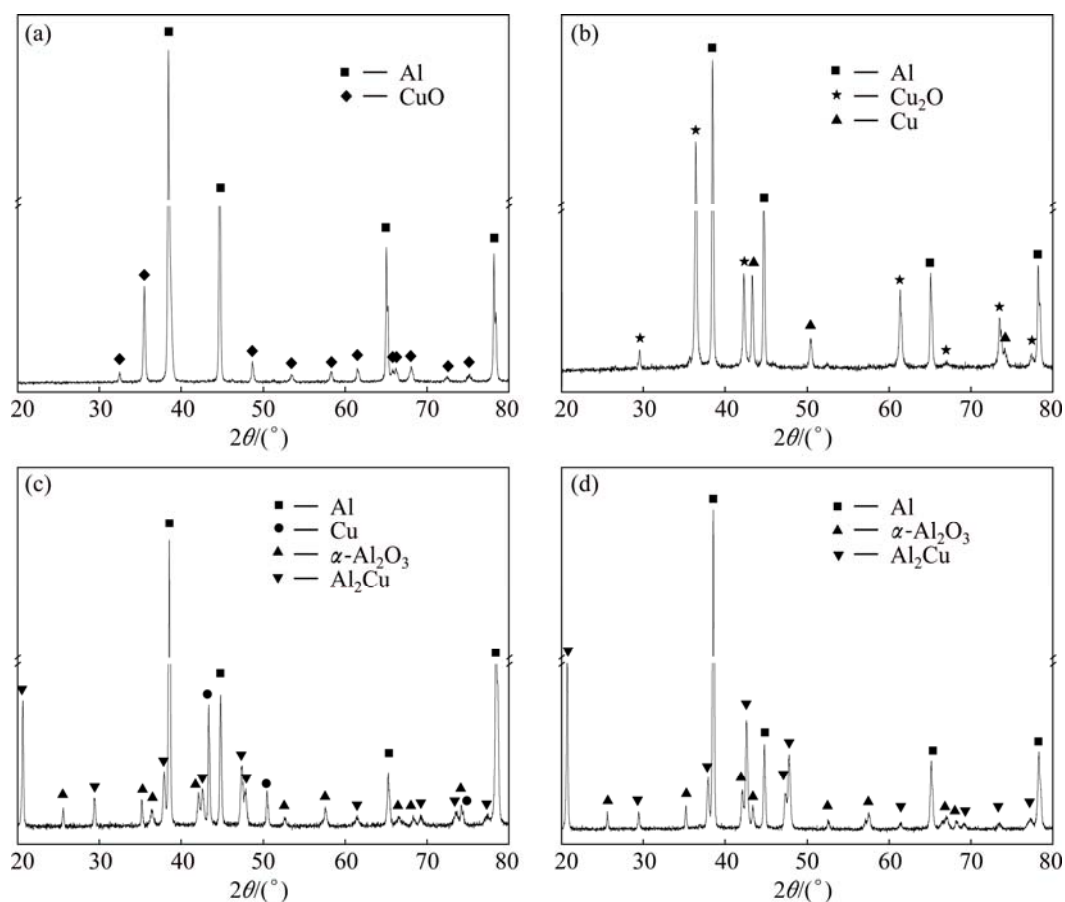


Fig. 2 XRD patterns of green sample and samples sintered at different temperatures for 1 h: (a) Green sample; (b) Sample 2 sintered at $600\text{ }^\circ\text{C}$; (c) Sample 1 sintered at $800\text{ }^\circ\text{C}$; (d) Sample 2 sintered at $700\text{ }^\circ\text{C}$

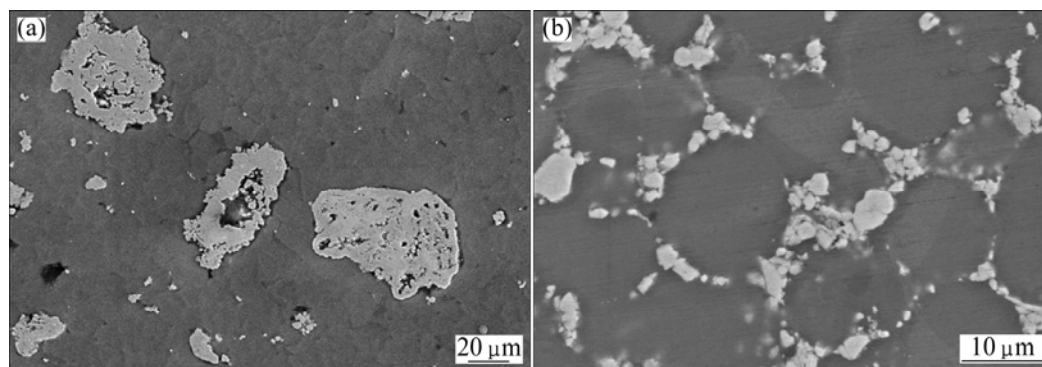


Fig. 3 SEM images of green samples made from CuO powders with different particle sizes: (a) Sample 1; (b) Sample 2

3.3.2 Incomplete reaction samples

The reaction between Al and CuO in sample 1 cannot completely be carried out before the temperature reaches 800 °C. Figure 4 shows the SEM image of sample 1 sintered at 800 °C and the corresponding EDS maps. According to the XRD result (Fig. 2(c)) and Fig. 3(a), it can be observed that most of the boundaries between Al particles disappear, but some of them form cracks. Al₂O₃ particles and unreacted Cu are distributed along the cracks.

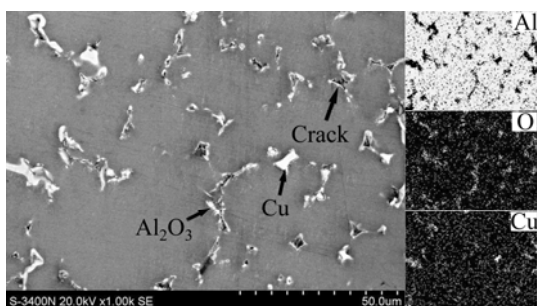


Fig. 4 SEM image of sample 1 sintered at 800 °C and corresponding EDS maps of elements Al, O and Cu

Figure 5 shows SEM image of sample 2 sintered at 600 °C and the corresponding EDS maps. The microstructure in Fig. 5 is similar to that of the green sample (Fig. 3(b)). According to the XRD pattern (Figs. 2(b)) and Fig. 3(b), it can be concluded that the bright patches are composites of Cu and Cu₂O. Some oxygen atoms are observed to be distributed along the boundaries between the Al particles, while others lie in the bright patches.

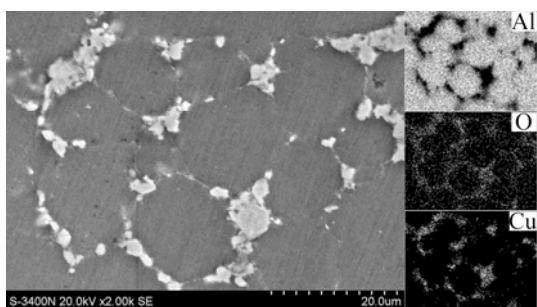


Fig. 5 SEM image of sample 2 sintered at 600 °C and corresponding EDS maps of elements Al, O and Cu

The reduction reaction between Al and CuO did not completely react and partial O atoms in CuO particles diffused along the Al particle surface and deposited on to the surface.

3.3.3 Complete reaction samples

According to the XRD results, the reactions between Al and CuO are complete in sample 1 sintered at 900 °C and sample 2 sintered at 700 °C. These two

samples have similar microstructures. Figures 6(a) and (b) show their microstructures, and an enlarged micrograph of sample 2 is shown in Fig. 6(c). The Al₂O₃ particles (bright dots) are observed to be distributed in the form of a network, with the distribution of the network similar to the boundaries between the Al particles in the green samples in Figs. 6(a) and (b). In addition, the block-like Al₂Cu phases are observed, and some Al₂O₃ particles are distributed around them. Figure 6(c) reveals that the morphology of Al₂O₃ particles is ribbon-like and their size is less than 2 μm. Cracks are observed, with some Al₂O₃ particles embedded in these cracks, and partial surfaces of these Al₂O₃ particles are not connected with the Al matrix.

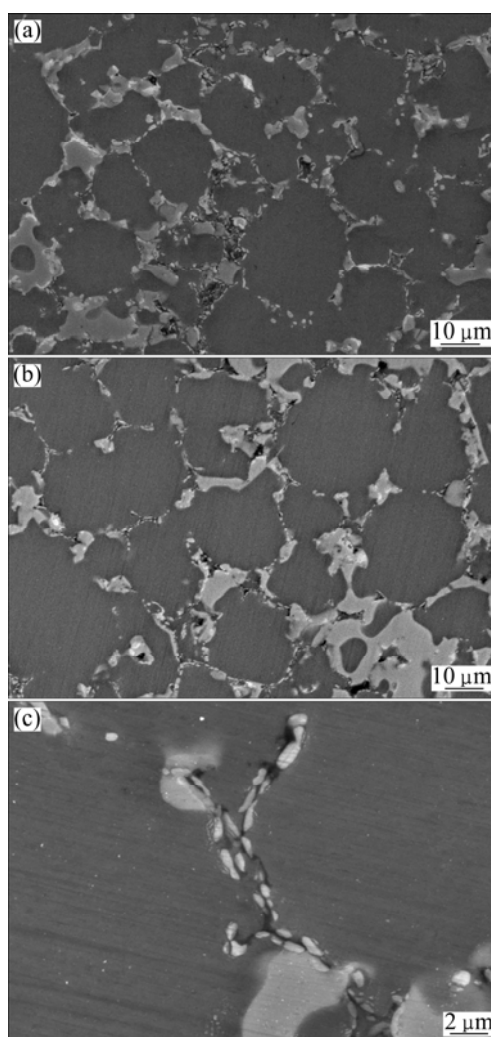


Fig. 6 SEM images of sintered samples: (a) Sample 1 sintered at 900 °C; (b) Sample 2 sintered at 700 °C; (c) Enlarged SEM image of sample 2 displaying detailed structures

The cracks of sample 1 disappear until the sintering temperature reaches 1000 °C, and the cracks of sample 2 disappear until the sintering temperature reaches 900 °C. These two samples have similar microstructures. Figures 7(a) and (b) show their microstructures, and an enlarged

micrograph of sample 2 is shown in Fig. 7(c). Al_2O_3 particles are not distributed in the form of a network. The morphologies of the Al_2O_3 particles are nearly spherical, and their size is observed to be less than approximately $2\ \mu\text{m}$.

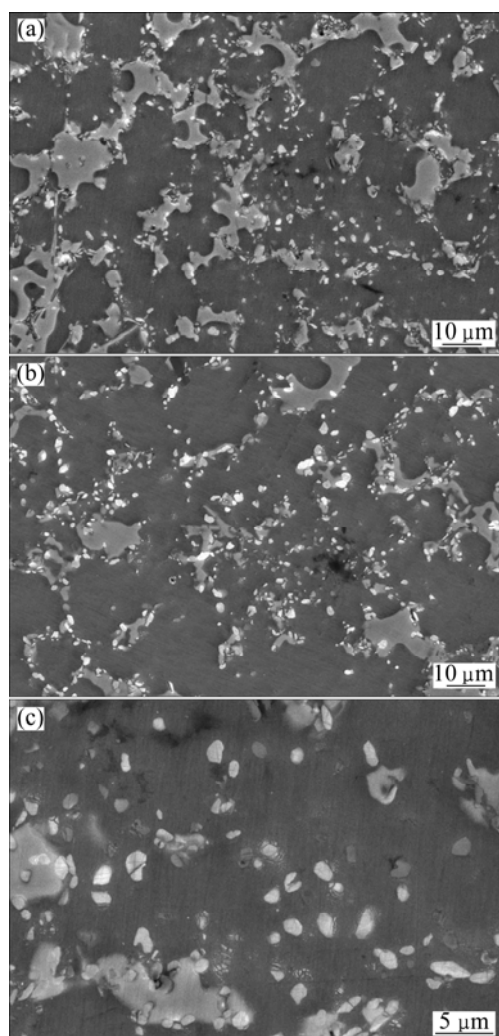


Fig. 7 SEM images of sintered samples: (a) Sample 1 sintered at $1000\ \text{°C}$; (b) Sample 2 sintered at $900\ \text{°C}$; (c) Enlarged SEM image of sample 2 displaying detailed structures of sample

3.4 Discussion

It is well known that the existence of an oxide film on the surface of the metal powder has a significant effect on the bonding properties of particles [21]. Once the film thickness is greater than a critical value, sintering between the particles will be obstructed. Oxygen atoms diffuse along the powder surfaces and the lattice and grain boundaries during sintering [12].

According to the above observation, the O atoms in CuO attach themselves to the Al particle surface at a low sintering temperature of $600\ \text{°C}$ in sample 2, while this phenomenon occurs in sample 1 sintered at $900\ \text{°C}$; in contrast, the O atoms in CuO only deposit onto the partial surface of Al particles in sample 1 sintered below

$800\ \text{°C}$, which indicates that the CuO particle size influences the diffusion rate of the O atoms in the CuO particles, i.e., the O atoms in tiny CuO particles have a faster diffusion rate and easily diffuse along the Al particle surface and deposit onto it.

The oxide film is formed on the surface of the Al particles and it acts as obstacles for the interconnection between molten Al particles. In addition, the cracks between Al particles in the green samples are not eliminated. Thus, Al_2O_3 particles are formed in the oxygen-rich region of the Al particle surface during sintering, the partial surface of the Al_2O_3 particles bonds with the Al matrix, and the other partial surface remains as a free surface when the sintering temperature is below a critical value. This phenomenon can also explain the reason for the Al_2O_3 particles to be distributed along the boundaries of the Al particles.

The free surfaces of the Al_2O_3 particles combine with Al matrix at high temperature, which may be explained by the wettability of the particles to Al, i.e., according to ZHOU et al [22] and KSIAZEK et al [23], the wetting of liquid Al with the Al_2O_3 particle surface increases with increasing temperature. The molten Al particles interconnect to each other to form molten aluminum. The re-distribution of Al_2O_3 particles is the result of their Brownian movement in molten aluminum, and the morphology of the Al_2O_3 particles varies from ribbon-like to nearly spherical in our sintered sample after the wetting of liquid Al with the Al_2O_3 particles.

4 Conclusions

1) Al_2O_{3p} -Al composites were synthesized in the 80%Al-20%CuO system. The particle size of CuO powders has a significant effect on the temperature at which complete reaction between Al and CuO occurs, but it has a relatively weak effect on the temperatures at which Al_2O_3 particles become spheroidized and the complete bonding between Al_2O_3 particles and Al matrix occurs.

2) When the size of the CuO particles is less than $100\ \mu\text{m}$, the temperature at which complete reaction between Al and CuO occurs is $900\ \text{°C}$. The Al_2O_3 particles bond with the Al matrix and exhibit the shape varying from ribbon-like to nearly spherical at $1000\ \text{°C}$.

3) When the size of CuO particles is less than $6\ \mu\text{m}$, the temperature at which complete reaction between Al and CuO occurs is $700\ \text{°C}$. The Al_2O_3 particles bond with the Al matrix and exhibit the shape varying from ribbon-like to nearly spherical at $900\ \text{°C}$.

References

- [1] WU C M L, HAN G W. Synthesis of an $\text{Al}_2\text{O}_3/\text{Al}$ co-continuous

- composite by reactive melt infiltration [J]. *Mater Charact*, 2007, 58: 416–422.
- [2] HESABI RAZAVI Z, SIMCHI A, REIHANI SEYED S M. Structure evolution during mechanical milling of nanometric and micrometric Al_2O_3 reinforced Al matrix composites [J]. *Mater Sci Eng A*, 2006, 428: 159–168.
- [3] RAHIMI M, EHASANI N, PARVIN N, BAHARVANDI H R. The effect of particle size, sintering temperature and sintering time on the properties of Al– Al_2O_3 composites, made by powder metallurgy [J]. *J Mater Process Technol*, 2009, 209: 5387–5393.
- [4] TJONG S C, MA Z Y. Microstructural and mechanical characteristics of in situ metal matrix composites [J]. *Mater Sci Eng A*, 2000, 29: 49–113.
- [5] HUANG Z J, YANG B, CUI H, ZHANG J S. Study on the fabrication of Al matrix composites strengthened by combined in-situ alumina particle and in-situ alloying elements [J]. *Mater Sci Eng A*, 2003, 351: 15–22.
- [6] HOSEINI M, MERATIAN M. Fabrication of in-situ aluminum–alumina composite with glass powder [J]. *J Alloys Compd*, 2009, 471: 378–382.
- [7] ABDULHAQQ HAMID A, GHOSH P K, JAIN S C, RAY S. Influence of particle content and porosity on the wear behavior of cast in-situ Al(Mn)– Al_2O_3 (MnO₂) composite [J]. *Wear*, 2006, 260(4–5): 368–378.
- [8] TAVOOSI M, KARIMZADEH F, ENAYATI M H. Fabrication of Al–Zn/ α - Al_2O_3 nanocomposite by mechanical alloying [J]. *Mater Lett*, 2008, 62: 282–285.
- [9] RAFIEI M, ENAYATI M H, KARIMZADEH F. Mechanochemical synthesis of (Fe,Ti)₃Al– Al_2O_3 nanocomposite [J]. *J Alloys Compd*, 2009, 488: 144–147.
- [10] YANG B, SUN M, GAN G S, XU C G, HUANG Z J, ZHANG H B, FANG Z G Z. In-situ Al_2O_3 particle-reinforced Al and Cu matrix composites synthesized by displacement reactions [J]. *J Alloys Compd*, 2010, 494: 261–265.
- [11] CHAN G, SUN G X, ZHU Z G. On the chemical reactions to process particle reinforced Al–Cu alloy matrix composites [J]. *Mater Sci Eng A*, 1998, 251: 226–231.
- [12] BURAK D, MEHMET G. The effect of sintering time on synthesis of in-situ submicron α - Al_2O_3 particles by the exothermic reactions of CuO particles in molten pure Al [J]. *J Alloys Compd*, 2013, 551: 101–107.
- [13] SONG K X, XING J D, DONG Q M, LIU P, TIAN B H, CAO X J. Internal oxidation of dilute Cu–Al alloy powders with oxidant of Cu₂O [J]. *Mater Sci Eng A*, 2004, 380: 117–122.
- [14] ZAHID G H, AZHAR T, MUSADDIQ M, RIZVI S S, ASHRAF M, HUSSAI N, IQBAL M. In-situ processing and aging behaviour of an aluminium/ Al_2O_3 composite [J]. *Mater Des*, 2011, 32: 1630–1635.
- [15] ZHU H G, MIN J, LI J L, AI Y L, GE L Q, WANG H Z. In-situ fabrication of (α - Al_2O_3 + Al_3Zr)/Al composites in an Al–ZrO₂ system [J]. *Compos Sci Technol*, 2010, 70: 2183–2189.
- [16] YU P, DENG C J, MA N G, YAU M Y, NGDICKON H L. Formation of nanostructured eutectic network in α - Al_2O_3 reinforced Al–Cu alloy matrix composite [J]. *Acta Mater*, 2003, 51: 3445–3454.
- [17] LIAL H P, SEKHAR A J. The influence of the reactant size on the micropyretic synthesis of NiAl intermetallic compounds [J]. *J Mater Res*, 1995, 10(10): 2471–2480.
- [18] FAN T X, ZHANG D, YANG G, TOSHIYA S, MASSAKI N. Fabrication of in-situ Al_2O_3 /Al composite via remelting [J]. *J Mater Process Tech*, 2003, 51: 3445–3454.
- [19] YU P, DENG C J, MA N G, NGDICKON H L. A new method of producing uniformly distributed alumina particles in Al-based metal matrix composite [J]. *Mater Lett*, 2004, 58: 679–682.
- [20] BISWAS A, ROY S K, GURUMURTHY K R, PRABHU N, BANERJEE S. A study of self-propagating high-temperature synthesis of NiAl in thermal explosion mode [J]. *Acta Mater*, 2002, 50(4): 757–773.
- [21] XIE G Q, OSAMU O, SONG M H, KAZUO F, TETSUJI N. Behavior of oxide film at the interface between particles in sintered Al powders by pulse electric-current sintering [J]. *Metall Mater Trans A*, 2003, 34(3): 699–703.
- [22] ZHOU X B, de HOSSON J Th M. Reactive wetting of liquid metals on ceramic substrates [J]. *Acta Mater*, 1996, 44(2): 421–426.
- [23] KSIAZE M, SOBCZAK N, MIKULOWSKI B, RADZIWIŁŁ W, SUROWIAK I. Wetting and bonding strength in Al/ Al_2O_3 system [J]. *Mater Sci Eng A*, 2002, 324: 162–167.

CuO 颗粒粒度对 Al–CuO 体系合成 Al_2O_3 p–Al 复合材料反应温度和显微组织的影响

赵 鸽, 史志铭, 塔 娜, 张瑞英

内蒙古工业大学 材料科学与工程学院, 呼和浩特 010051

摘 要: 在 80%Al–20%CuO(质量分数)体系中, 通过原位反应法制备 Al_2O_3 p–Al 复合材料。采用不同方法研究 CuO 颗粒粒度对复合材料合成温度和显微组织的影响。结果表明, CuO 颗粒粒度对 Al–CuO 体系的完全反应温度有显著影响: 含有粒度小于 6 μm CuO 颗粒样品的完全反应温度比含有粒度小于 100 μm CuO 颗粒样品的完全反应温度低 200 $^\circ\text{C}$ 。当反应温度低于某一临界值时, 原位 Al_2O_3 颗粒和 Al 基体之间不能完全结合; 当温度高于某一临界值时, 原位 Al_2O_3 颗粒的形貌从棒状转变成近球形。这两个临界温度受 CuO 颗粒粒度的影响: 含有粒度小于 6 μm CuO 颗粒样品的临界温度比含有小于 100 μm CuO 颗粒样品的临界温度低 100 $^\circ\text{C}$ 。

关键词: CuO; 颗粒粒度; 反应温度; Al_2O_3 p–Al 复合材料

(Edited by Wei-ping CHEN)